Nuclear Instruments and Methods in Physics Research A 593 (2008) 544–549

Contents lists available at ScienceDirect

Nuclear Instruments and Methods in Physics Research A

journal homepage: www.elsevier.com/locate/nima

Electron irradiation effects on the organic-on-inorganic silicon Schottky structure

Ö. Güllü [a,*], Ş. Aydoğan [a], K. Şerifoğlu [b], A. Türüt [a]

[a] Department of Physics, Atatürk University, 25240 Erzurum, Turkey
[b] Radiation Oncology Department, Faculty of Medicine, Atatürk University, 25240 Erzurum, Turkey

ARTICLE INFO

Article history:
Received 20 April 2008
Received in revised form
12 May 2008
Accepted 26 May 2008
Available online 20 June 2008

Keywords:
Schottky barrier
Ideality factor
Series resistance
Electron irradiation

ABSTRACT

In this study, the effects of high-energy electron irradiation on the electrical characteristics of a Rhodamine-101(Rh101)/p-Si Schottky structure were investigated. Some contact parameters such as barrier height, ideality factor and series resistance were calculated from the current–voltage (*I*–*V*) characteristics. It was seen that these three parameters were increased by the electron irradiation. After the electron irradiation, it was also seen that the carrier concentration, the reverse bias current and the capacitance of the device decreased.

1. Introduction

Radiation effects in semiconductors are of concern for a broad range of device applications [1]. Thus, radiation plays a significant role in physical properties of materials. When an energetic electron beam passes through a material, different modifications occur, according to the properties of radiation. Also, the nature of odifications depends on the electrical, thermal, optical, structural and physical properties of the material, the mass of the projectile ion and its energy and also the type of irradiation like its fluency and beam dimension [2]. High-energy radiation penetrates the metal–semiconductor (MS) interface and causes damage deep below the interface. Low-energy radiation causes severe lattice damage in the form of vacancies, interstitials and defect complexes at the near interface of the device [3–6]. The one kind of the radiation is electron beam, which is accelerated. Mills [7] was the first to recognize that electrons with an energy of 1 MeV would posses enough energy to displace an atom from its lattice position. This observation has led to the increased use of electron accelerators in radiation damage studies. This use has been motivated by two important facts. First, electron bombardment experiments permit the determination of the energy required to remove an atom from its initial position. This is done by increasing the energy of the electrons until an observable change in a radiation-sensitive property is seen. The second important basis for the use of electrons lies in the fact that as long as the energy of the electrons is close to the displacement threshold, it is presumed that only single Frenkel pairs are formed. Thus, many radiation-induced phenomena can be analyzed in terms of a single vacancy and/or interstitial atom, and one avoids the complication attendant upon the generation of complex damage regions presumed to occur in heavy-charged particle irradiation. As a result of these two circumstances, electron irradiation forms a valuable supplement to other techniques [8].

Rectifying MS contacts are basic devices in the technology of semiconductors. In a Schottky diode some parameters, such as ideality factor, barrier height (BH) and series resistance, affect the performance of the device. These parameters give useful information concerned with the nature of the diode. In most MS contacts, there is a native thin oxide layer on the surface of the semiconductor unavoidably. This layer converts the MS structure into a metal/interlayer/semiconductor (MIS) device. In this way, Schottky BHs of the MS contacts can be manipulated by the insertion of a dipole layer (Rhodamine-101(Rh101) organic layer) between the semiconductor and the metal [9–11]. Recently, investigations of a new class of MIS structures, i.e. metal/organic/inorganic semiconductor structures, have attracted much interest due to both the unusual nature of these contacts and the potential new optical and electronic devices can be applied. In particular, molecular organic semiconductors exhibit rectification, when deposited onto inorganic semiconductor substrates. On the other hand, some semiconductors such as Si and GaAs have been successfully applied in solar energy conversion because of the wide absorption band in the visible spectral region [12].

* Corresponding author. Tel.: +90 442 231 4081; fax: +90 442 236 0948.
E-mail address: omergullu@gmail.com (Ö. Güllü).

0168-9002/$ - see front matter
doi:10.1016/j.nima.2008.05.043

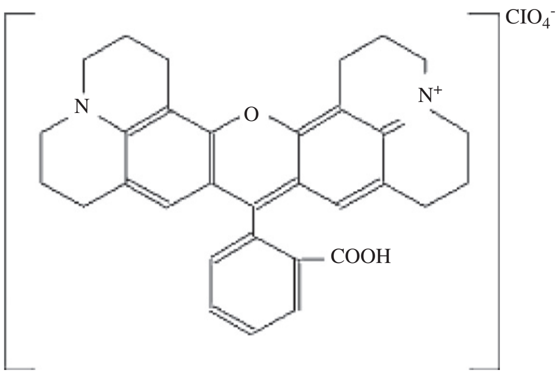

Fig. 1. Chemical structure of Rh101

Rhodamine 101 (Rh101) has the molecule formula $C_{32}H_{30}N_2O_3$. The Rh101 is a xanthene-type organic molecule, and has a molecular fluorescence quantum yield close to unity, being independent of temperature. Its appearance is green solid. Rh101 is a well-known organic laser dye, indicating the absence of any transient absorption in the spectral region of the emission spectrum [13]. The molecule structure of the Rh101 is shown in Fig. 1. The presence of such an interfacial layer at the MIS structures makes it rather sensitive to irradiation. It is known that electron irradiation can generate electronic states at the inorganic–organic (such as Si- Rh101) interface in MIS structures. Exposure of the MIS structures to electron irradiation will cause electron–hole pair generation and changes in the crystal lattice. When the MIS structures are stressed with an external bias, these electron–hole pairs would be separated by the strong local internal electric field at interface. The electrons are swept out of the organic interlayer (Rh101) quickly by the electric field while the holes slowly and could also be trapped by the defects [6].

Pb/Rh101/p-Si MIS devices can be attractive for space applications. Stability against particle irradiation is essential for the long-term suitability of MIS structures for space applications. In the space environment, the devices are constantly subjected to electron bombardment of high (MeV) energy. Electron irradiation is known to have less degradation effect than neutron irradiation of similar energy and dose, but have a higher damage coefficient than for gamma rays. Radiation causes ionization and atomic displacement in semiconductors. MIS devices are damaged principally by the displacement of atoms from native sites to form defects [14]. For this purpose, investigation was carried out of the effects of high-energy electron irradiation with an electron fluency of $3\times10^{12}\,e^-/cm^2$ on the Pb/Rhodamin-101/p-Si structure parameters.

2. Experimental procedure

We have used a p-type Si semiconductor wafer with (1 0 0) orientation and 400 μm thickness and 1–10 Ω cm resistivity. Before making contacts, the wafer was chemically cleaned using the RCA cleaning procedure (i.e. 10 min boiling in NH_3+H_2O_2+6H_2O followed by a 10 min HCl+H_2O_2+6H_2O at 60 °C). The ohmic contact with a thickness of 120 nm was made by evaporating the Al metal on the back of the p-Si substrate, and then was annealed at 580 °C for 3 min in N_2 atmosphere. The native oxide on the front surface of the substrate was removed in HF+10H_2O solution. Finally, it was rinsed in deionised water for 30 s, and then was dried. The Rh101 organic layer with a thickness of 40 nm was directly formed on the front surface of the p-Si wafer. Then, Pb was evaporated on the Rh101 layer at 10^{-5} torr (diode area $= 7.85\times10^{-3}\,cm^2$). Thickness of the Pb top contact was 80 nm. The current–voltage (I–V) and capacitance–voltage–frequency (C–V–f) measurements of the Pb/Rh101/p-Si structure under 6 MeV-energy electron irradiation with a fluency of $3\times10^{12}\,e^-/cm^2$ were performed with a KEITLEY 487 Picoammeter/Voltage Source and an HP 4192 A (5 Hz–13 MHz) LF IMPEDENCE ANALYZER, respectively, at room temperature. No bias voltage was applied to the device during the irradiation.

3. Results and discussion

For a Schottky diode, the thermionic-emission theory (TE) predicts that the I–V characteristics at forward biases are expressed by [10]

$$I = AA^*T^2 \exp\left(-\frac{q\Phi_b}{kT}\right)\left[\exp\left(\frac{qV}{nkT}\right) - 1\right] \tag{1}$$

where

$$I_0 = AA^*T^2\left(-\frac{q\Phi_b}{kT}\right) \tag{2}$$

is the saturation current, Φ_b is the effective BH at zero bias, A^* is the Richardson constant and equals to 32 A cm^{-2} K^{-2} for p-type Si, where q is the electron charge, V is the applied voltage, A is the diode area, k is Boltzmann's constant, T is the temperature in Kelvin, n is the ideality factor, and it is determined from the slope of the linear region of the forward-bias ln I–V characteristic through the relation

$$n = \frac{q}{kT}\frac{dV}{(\ln I)} \tag{3}$$

n equals to one for an ideal diode. However, n has usually a value greater than unity. High values of n can be attributed to the presence of the interfacial thin layer, a wide distribution of low-SBH patches (or barrier inhomogeneities) and to the bias voltage dependence of the SBH [10].

Φ_b is the zero-bias BH, which can be obtained from the following equation

$$\Phi_b = kT/q\ln(AA^*T^2/I_0). \tag{4}$$

Fig. 2 depicts the forward and reverse bias I–V characteristics of the Pb/Rh101/p-Si/Al structure for unirradiated and irradiated cases by 6 MeV energy electron irradiation with $3\times10^{12}\,e^-/cm^2$. It is seen that the electron irradiation causes a significant reduction in both forward and reverse current. The radiation-induced degradation observed in the reverse I–V characteristics could be attributed to an increase in interfacial defect density [15]. The values of the BHs for before and after irradiation were calculated as 0.72 and 0.75 eV, respectively. Furthermore, the values of the ideality factors for before and after irradiation were extracted as 2.82 and 3.14, respectively. The high values in the ideality factor are possibly caused by an organic interlayer plus a native oxide film between the top metal and the inorganic semiconductor. It was seen that the BH and the ideality factor increased by electron irradiation. This may be due to the introduction of irradiation-induced defects at the interface between the Rh101 layer and the p-Si substrate. The irradiation of materials by high-energy particles is known to introduce lattice defects and the semiconductor properties are sensitive to defect concentrations [16]. The cause of decrease in both reverse and forward current is attributed to the creation of the deep-level defect act as the center of the carrier recombination at the interface. This change indicates a change in electrical properties of the interface, including the possibility of chemical intermixing, which can change the location of Fermi energy level pinning for the device. Besides, the increase in the n and Φ_b indicate that after irradiation, the current

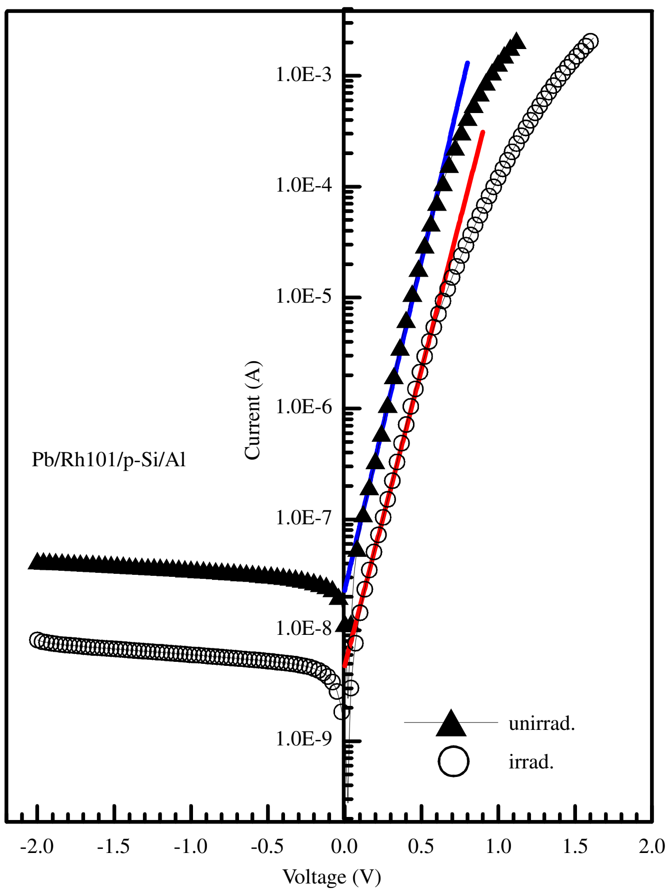

Fig. 2. The I–V characteristics of the Pb/Rh101/p-Si/Al structure

transport mechanism was deviated from thermionic-emission theory.

The forward-bias I–V characteristics of the Pb/Rh101/p-Si Schottky devices are linear but deviate considerably from linearity due to the some factors at large voltages. One of these factors is series resistance (R_s). The series resistance is an important parameter on the electrical characteristics of Schottky barrier contacts. R_s is influenced by the presence of the interface layer between the metal and the semiconductor and leads to non-ideal forward-bias current–voltage plots. When the applied voltage is sufficiently large, the effect of the R_s can be seen at the non-linear regions of the forward-bias I–V characteristics. The Schottky diode parameters as the BH, the ideality factor and the series resistance can also be achieved using a method developed by Cheung and Cheung [17].

According to Ref. [17], the forward-bias I–V characteristics due to the TE of a Schottky diode with the series resistance can be expressed as

$$I = I_0 \exp\left[\frac{q(V - IR_s)}{nkT}\right] \tag{5}$$

where the IR_s term is the voltage drop across series resistance of the device. The values of the series resistance can be determined from the following functions using Eq. (5):

$$\frac{dV}{d(\ln I)} = \frac{nkT}{q} + IR_s \tag{6}$$

$$H(I) = V - \left(\frac{nkT}{q}\right)\ln\left(\frac{I}{AA^*T^2}\right) \tag{7}$$

and $H(I)$ is given as follows:

$$H(I) = n\Phi_b + IR_s. \tag{8}$$

A plot of $dV/d(\ln I)$ vs. I will be linear and gives R_s as the slope and nkT/q as the y-axis intercept from Eq. (6). Fig. 3 shows the plots of $dV/d(\ln I)$ vs. I for unirradiated and irradiated cases. The values of n and R_s were calculated as $n = 3.23$, $R_s = 106\,\Omega$ before electron irradiation and $n = 4.42$, $R_s = 111\,\Omega$ for after one, respectively. It is seen that the value of n obtained from the forward-bias $\ln I$–V plot is smaller than that of the $dV/d(\ln I)$–I curves. This can be attributed to the effect of the series resistance and interface states and to the voltage drop across the interfacial organic layer.

Besides, the $H(I)$ vs. I plot has to be linear according to Ref. [18]. The slope of this plot gives a different determination of R_s. Using the value of n obtained from Eq. (8), the value of Φ_b was obtained from the y-axis intercept. The $H(I)$ vs. I curves are shown in Fig. 4. From the $H(I)$ vs. I plots, the values of the Φ_b and R_s were calculated as $\Phi_b = 0.81$ eV, $R_s = 129\,\Omega$ for the unirradiated device and $\Phi_b = 0.83$ eV, $R_s = 152\,\Omega$ for the irradiated one.

Norde proposed an alternative method to determine the value of the series resistance [18]. The following function has been defined in the modified Norde's method:

$$F(V) = \frac{V}{\gamma} - \frac{kT}{q}\ln\left(\frac{I(V)}{AA^*T^2}\right) \tag{9}$$

where γ is the first integer (dimensionless) greater than the ideality factor. $I(V)$ is current obtained from the I–V curve. Once the minimum of the F vs. V plot is determined, the value of BH can be obtained from Eq. (10), where $F(V_0)$ is the minimum point of $F(V)$ and V_0 is the corresponding voltage.

$$\Phi_b = F(V_0) + \frac{kT}{q}. \tag{10}$$

Fig. 5 shows the $F(V)$–V plot of the junction. From Norde's functions, R_s value can be determined as

$$R_s = \frac{kT(\gamma - n)}{qI}. \tag{11}$$

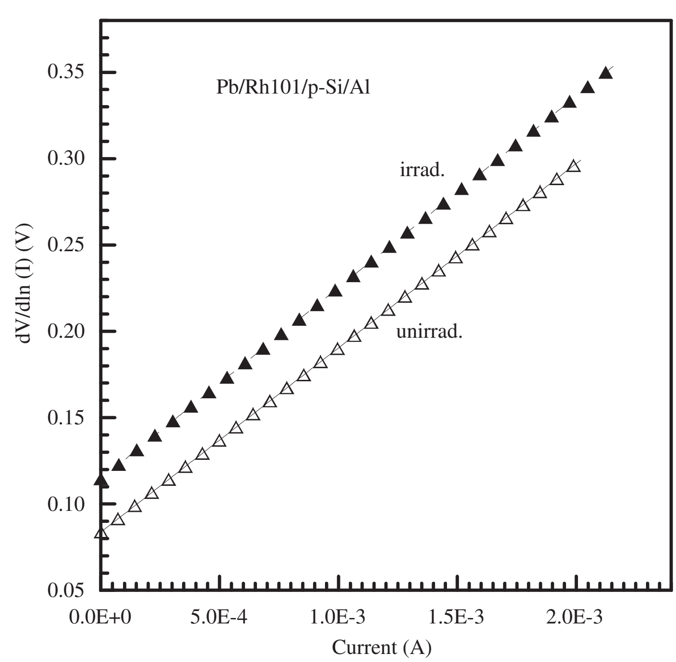

Fig. 3. A plot of $dV/d(\ln I)$ vs. I obtained from forwar bias I–V characteristics of the Pb/Rh101/p-Si/Al structure for before and after electron irradiation conditions.

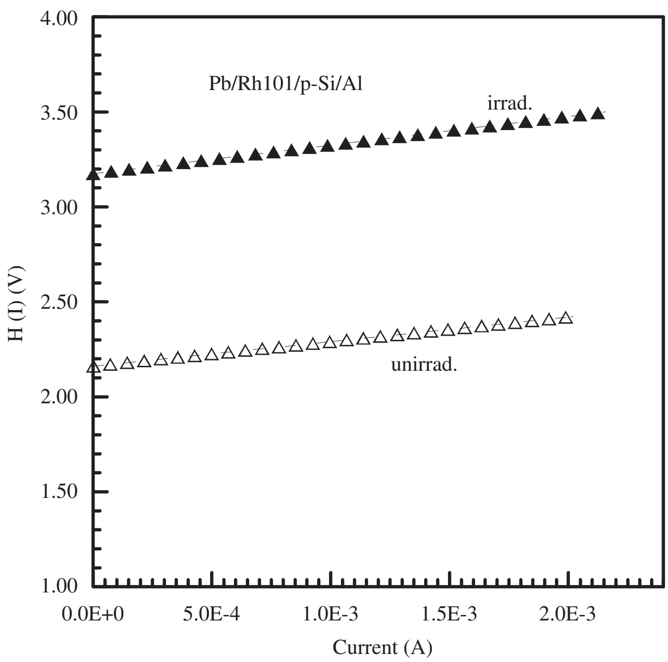

Fig. 4. A plot $H(I)$ vs. I obtained from forward bias I–V characteristics of the Pb/Rh101/p-Si/Al structure for before and after electron irradiation.

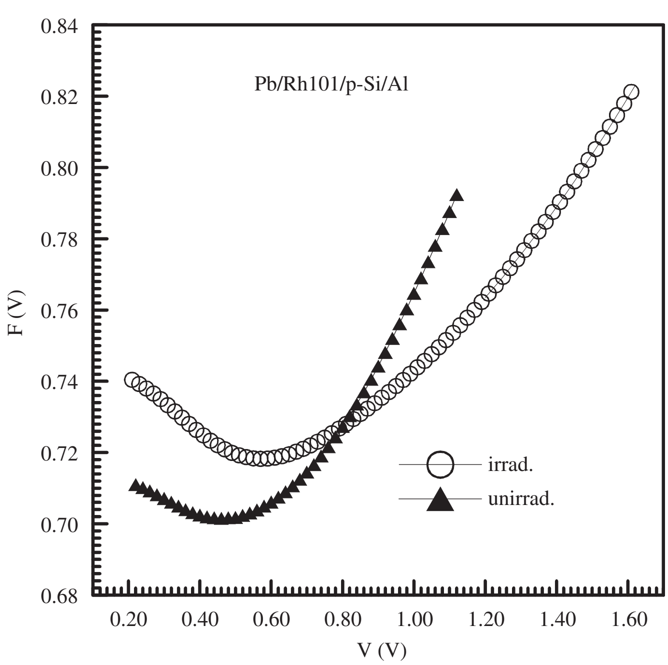

Fig. 5. $F(V)$ vs. V plots of the Pb/Rh101/p-Si/Al structure for unirradiated and irradiated cases.

From the F–V plot the values of Φ_b and R_s of the structure were determined as 0.82 eV and 328 Ω for the unirradiated diode, and as 0.84 eV and 453 Ω for the irradiated case, respectively. It was seen that the values of R_s obtained from both Cheung and Norde methods increased by the applied electron radiation. An increase in series resistance indicates that the product of the mobility and the free carrier concentration has reduced. The reduction in mobility is due to the introduction of defect centers on irradiation, which act as scattering centers [14].

The analysis of the C–V characteristics was achieved by using the following equation:

$$C^{-2} = \frac{2(V_d + V)}{\varepsilon_s \varepsilon_0 q A^2 N_a} \tag{12}$$

where V_d is the diffusion potential at zero bias, which is determined from the extrapolation of the linear $1/C^2$–V plot to the V axis, A is the effective area of the diode and ε_s is the dielectric constant of the semiconductor (= 11.7 for Si [19] and N_a is the concentration of ionized acceptors. The value of the BH Φ_b can be calculated by the following well-known equation, using the C–V measurements:

$$\phi_b = V_d + V_p \tag{13}$$

where V_p is the potential difference between the Fermi energy level (E_f) and the top of the valance band in the neutral region of p-Si, which is directly equal to E_f, and can be calculated by knowing N_a and N_v, density of states in the valance band, which is $N_v = 1.04 \times 10^{19}\,\text{cm}^{-3}$ for p-Si at room temperature [19].

Figs. 6 and 7 show the typical C–V characteristics for unirradiated and irradiated structures at various frequencies. It is seen from these figures that the values of the capacitance decrease by irradiation and with frequency. This decrease can be attributed to the change in dielectric constant at the metal–semiconductor interface or to the decrease in the net ionized dopant concentration by electron irradiation [5,19,20].

Fig. 8 depicts the reverse bias C^2–V characteristics of the Pb/Rh101/p-Si/Al structure only at $f = 500$ kHz frequency. It is seen that the intercept of the C^2–V characteristics after irradiation shifts towards more positive voltages while the gradient remains almost constant. The shift in the C^2–V characteristics is due to the increase in diffusion potential, which results from an increase in the BH. The acceptor (N_a) doping concentrations were found as 6.62×10^{14} and $2.27 \times 10^{14}\,\text{cm}^{-3}$ for before and after electron irradiation, respectively, at 500 kHz frequency using the following equation:

$$N_a = N_v \exp(V_p/kT). \tag{14}$$

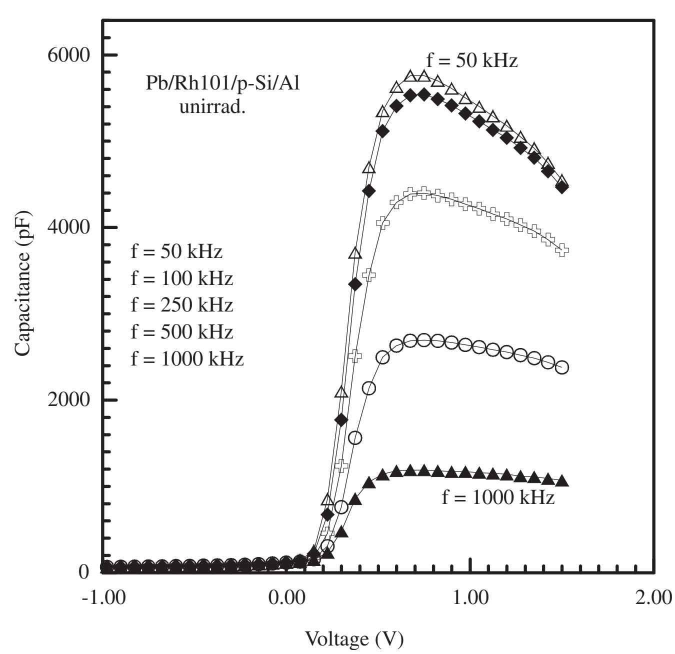

Fig. 6. The forward and reverse bias C–V characteristics of the Pb/Rh101/p-Si/Al structure before electron irradiation at various frequencies.

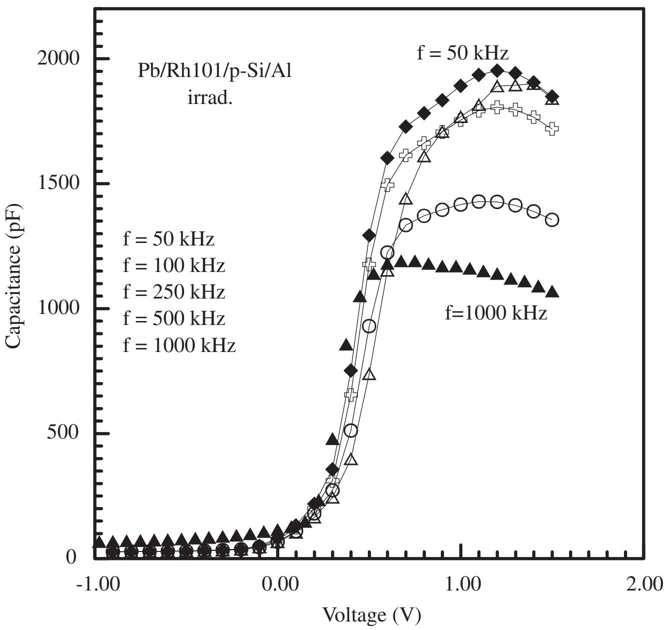

Fig. 7. The forward and reverse bias C–V characteristics of the Pb/Rh101/p-Si/Al structure after electron irradiation at various frequencies.

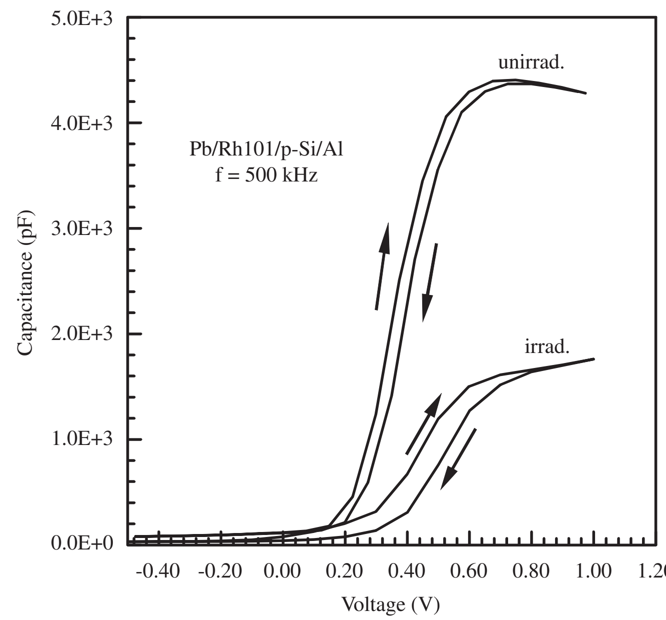

Fig. 9. The forward and reverse bias MIS C–V characteristics of the Pb/Rh101/p-Si/Al structure for before and after electron irradiation at $f = 500$ kHz frequency.

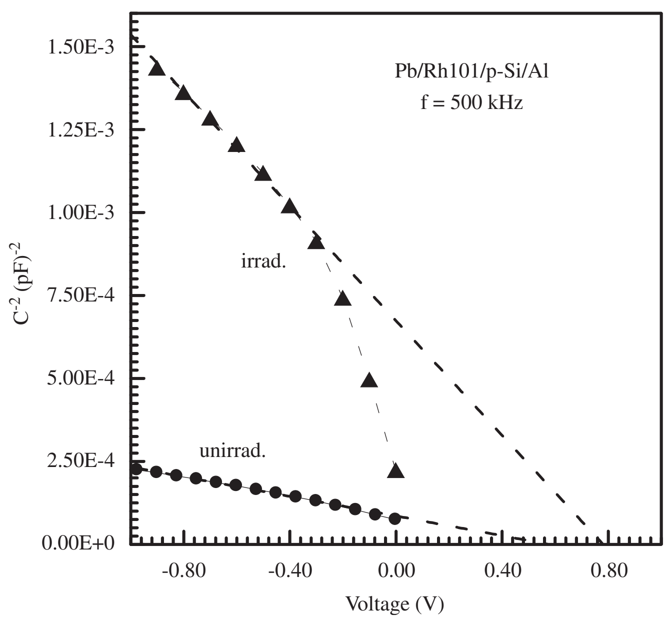

Fig. 8. The forward and reverse bias C^{-2}–V characteristics of the Pb/Rh101/p-Si/Al structure before and after electron irradiation at $f = 500$ kHz frequency.

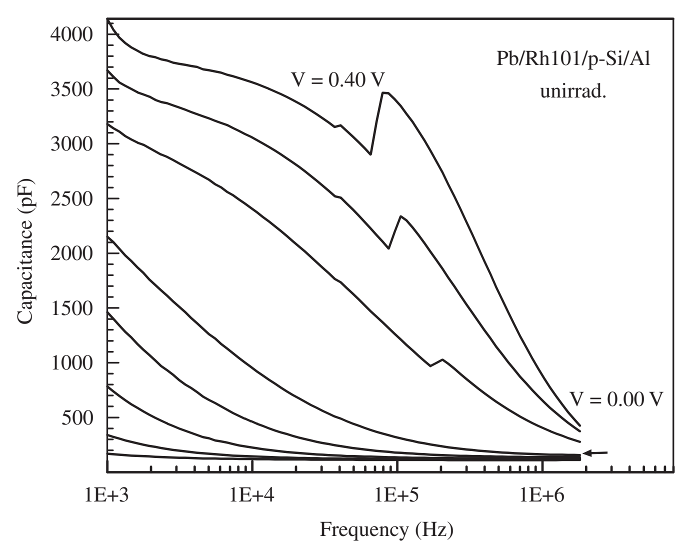

Fig. 10. The forward bias C–f characteristics of the Pb/Rh101/p-Si/Al structure before electron irradiation at various voltages.

The possible reason of this reduction in carrier density may be that substitutional acceptors are moved into the interstitial site or the creation of hole capture levels or donor-like defects at the interface of Rh101 and p-Si.

The values of the BHs obtained from the reverse bias C^{-2}–V characteristics at 500 kHz frequencies have been found as 0.82 and 1.10 eV for before and after irradiation, respectively. The values of the BHs extracted from the C–V curves are higher than those derived from the I–V measurements. This difference can be explained due to an interface layer or the barrier inhomogeneities [21].

Fig. 9 shows the C–V characteristics of MIS capacitor properties for the structure at $f = 500$ kHz frequency, both before and after irradiation. The C–V hysteresis in the structure is attributed to electron charging and discharging by tunneling though the organic layer between the Pb and p-Si. It can be noticed that decrease in both the capacitance and doping concentration is in the same ratio (about 1/3 ratio) for unirradiated and irradiated values. These results show that the electron irradiation generates positive charges between the Rh101 and p-Si interface.

Figs. 10 and 11 show the capacitance–frequency (C–f) characteristics for unirradiated and irradiated conditions of the structure at various voltages. It is seen from these figures that the values of the capacitance decrease by irradiation. As described above, this can be attributed to the change in the dielectric constant at the interface and/or to the decrease in the net ionized dopant concentration with electron irradiation. Besides, the higher values of capacitance at low frequency are due to the excess capacitance resulting from the interface states in equilibrium with the p-Si that can follow the alternating current signal. The interface states at lower frequencies follow the alternating

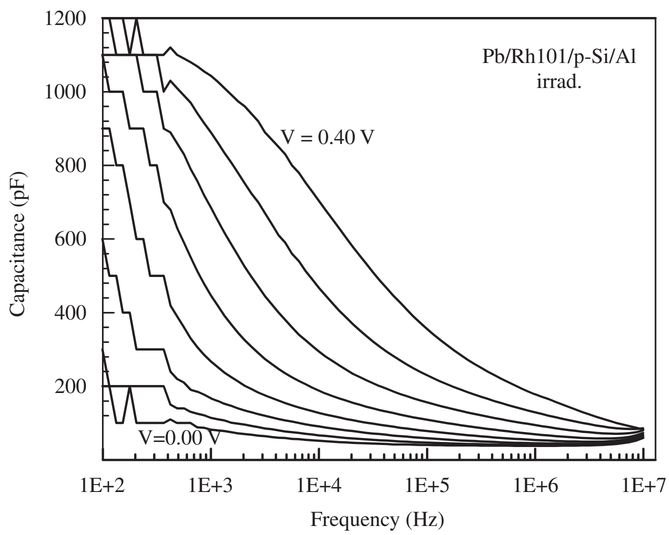

Fig. 11. The forward bias *C–f* characteristics of the Pb/Rh101/p-Si/Al structure after electron irradiation at various voltages.

current signal, whereas at higher frequencies they cannot follow the alternating current signal. The values of the capacitance at the high-frequency region originate from only space charge capacitance.

4. Conclusion

In conclusion, a Pb/Rh101/p-Si/Al structure was fabricated and the effect of 6 MeV-electron irradiation on the electrical characteristics of the structure was investigated. It was seen that after electron irradiation the BH values, the series resistance values and ideality factors increased. Furthermore, it was seen that the capacitance values increased after electron irradiation. This was attributed to the change in dielectric constant at the interface and/or to decrease in the net ionized dopant concentration and the interface states. The degradation of the diode properties may be due to the introduction of electron irradiation-induced interfacial defects via displacement damage.

References

[1] T.R. Weatherford, W.T. Anderson, IEEE Trans. Nucl. Sci. NS-50 (3) (2003) 704.
[2] J.P. Singh, R. Singh, S. Ghosh, A. Tripathi, D. Kabiraj, S. Gupta, T. Som, R. Kumar, S.K. Arora, K. Asokan, D.K. Avasthi, D. Kanjilal, N.C. Mishra, G.K. Metha, Nucl. Instr. and Meth. B 156 (1999) 206.
[3] S.T. Li, B.D. Nener, I. Faraone, A.G. Nassibuan, M.A.C. Hotchkis, J. Appl. Phys. 73 (1993) 640.
[4] S. Arulkumaran, J. Arokiaraj, N. Dharmarasu, J. Kumar, Nucl. Instr. and Meth. B 119 (1996) 519.
[5] Ö. Güllü, F. Demir, F.E. Cimilli, M. Biber, Vacuum 82 (2008) 789; Ö. Güllü, M. Çankaya, M. Biber, A. Türüt, J. Phys. D: Appl. Phys. 41 (2008) 135103.
[6] A. Tataroglu, S. Altindal, M.M. Bulbul, Nucl. Instr. and Meth. A 568 (2006) 863; M. Gökçen, A. Tataroğlu, Ş. Altındal, M.M. Bülbül, Radiat. Phys. Chem. 77 (2008) 74.
[7] M. Mills, Unpublished work. His calculations first showed the possibility of using electrons for radiation damage studies.
[8] S. Billington, H. Crawford, Radiation Damage in Solids, Princeton University Press, 1961.
[9] S.M. Sze, Physics of Semiconductor Devices, second ed, Wiley, New York, 1981.
[10] E.H. Rhoderick, R.H. Williams, Metal–Semiconductor Contacts, Clarendon Press Oxford, 1988.
[11] R.H. Williams, G.Y. Robinson, in: C.W. Wilmsen (Ed.), Physics and Chemistry of III–V Compound Semiconductor Interfaces, Edited by Plenum Press, New York, 1985.
[12] S. Darwish, Egypt. J. Sol. 26 (1) (2003) 55.
[13] O. Vural, N. Yıldırım, S. Altındal, A. Türüt, Synth. Met. 157 (2007) 679.
[14] M. Pattabi, S. Krishnan, Ganesh, X. Mathew, Sol. Energy 81 (2007) 111.
[15] G.A. Umana-Membreno, J.M. Dell, G. Parish, B.D. Nener, L. Faraone, U.K. Mishra, IEEE Trans. Electron Devices 50 (2003) 12.
[16] S.A. Goodman, F.D. Auret, M. du, Plessis, W.E. Meyer, Semicond. Sci. Technol. 14 (1999) 323.
[17] S.K. Cheung, N.W. Cheung, Appl. Phys. Lett. 49 (1986) 85.
[18] S. Karatas, S. Altindal, A. Turut, M. Cakar, Physica B 392 (2007) 43.
[19] S. Karatas, A. Turut, Nucl. Instr. and Meth. A 566 (2006) 584.
[20] P. Zukowski, J. Partyka, P. Wegierek, Phys. Stat. Sol. A 159 (1997) 509.
[21] C. Coskun, S. Aydogan, H. Efeoglu, Semicond. Sci. Technol. 19 (2004) 242.